ORNL/SPR-2024/3593
M3LW-24OR0402015

Light Water Reactor Sustainability Program

Analysis of attenuation effects based on results from Zion beltline reactor pressure vessel

Mikhail A. Sokolov and Roger Stoller
Oak Ridge National Laboratory

September 2024

U.S. Department of Energy
Office of Nuclear Energy

Light Water Reactor Sustainability Program
Materials Research Pathway
Milestone Report: M3LW-24OR0402015

ANALYSIS OF ATTENUATION EFFECTS BASED ON RESULTS FROM ZION BELTLINE REACTOR PRESSURE VESSEL

Mikhail A. Sokolov and Roger Stoller

Oak Ridge National Laboratory

September 2024

Prepared by
OAK RIDGE NATIONAL LABORATORY
Oak Ridge, TN 37831-6283
managed by
UT-BATTELLE LLC
for the
US DEPARTMENT OF ENERGY
under contract DE-AC05-00OR22725

CONTENTS

List of Figures

List of Tables

ACKNOWLEDMENT

This research was sponsored by the U.S. Department of Energy, Office of Nuclear Energy, Light Water Reactor Sustainability Program Materials Research Pathway under contract DE-AC05-00OR22725 with UT-Battelle, LLC / Oak Ridge National Laboratory. The authors wish to thank Dr. Tim Lach and Dr. Wei Tang who reviewed this report. Continuous support from Xiang (Frank) Chen and Thomas Rosseel, the current and former, Program Managers of the Materials Research Pathway of the Light Water Reactor Sustainability Program is highly appreciated.

EXECUTIVE SUMMARY

The decommissioning of the Zion Units 1 and 2 Nuclear Generating Station in Zion, Illinois, presented a unique opportunity for developing a better understanding of materials degradation and other issues associated with extending the lifetime of existing nuclear power plants (NPPs) beyond 60 years of service. In support of extended service and current operations of the US nuclear reactor fleet, the Oak Ridge National Laboratory (ORNL), through the Department of Energy (DOE), Light Water Reactor Sustainability (LWRS) Program Materials Research Pathway, coordinated with Zion Solutions, LLC, a subsidiary of Energy Solutions (ES), the selective procurement of materials, structures, and components, from the decommissioned reactors including multiple segments of the Zion Unit 1 Reactor Pressure Vessel (RPV).

As described in the previous LWRS milestone reports [1-9], the LWRS Materials Research Pathway acquired four reactor pressure vessel (RPV) segments that were harvested (December 2015) from the Zion Unit 1 NPP and shipped by rail (April 2016) to the Energy Solutions (ES) Memphis Processing Facility (MPF) in Memphis, Tennessee [1]. At the MPF, the Zion Unit 1 RPV ORNL Beltline Weld Segment 1 was cut into seven blocks (September 2016): five base metal and two beltline welds from the high fluence region of the segment [2]. Upon completion of the cutting operation, the seven blocks were packaged and transferred to BWX Technologies, Inc. (BWXT), Lynchburg, VA (October 2016) and the cutting waste and unused RPV segments shipped to the ES waste disposal site in Clive UT (December 2016) [3]. The machining of through-wall test specimens was performed at BWXT, Lynchburg, VA [4]. Finally, the initial testing of the Zion Harvesting Project (ZHP) was completed as described in [5-7]. It included Charpy impact data, fracture toughness, chemical analysis, and Atom Probe Tomography characterization of the beltline materials. Based on these results, it was determined that acquiring archive material to obtain through-thickness properties variations can be properly accounted for in the evaluation of radiation embrittlement. As part of the industry engagement efforts, discussions were held with the PWR Owners Group (PWROG). As result of these efforts, the PWROG agreed that Westinghouse would provide an archived piece of Zion material that contains both base and weld metals [8-9].

One of the unique opportunities of harvesting through thickness beltline material from previously operated plant was possibility to access the potential effects of attenuation on degradation of mechanical properties of RPV materials. This report describes the results of the evaluation of potential attenuation effects using characterization results of Zion beltline materials. This report was prepared in satisfaction of Milestone M3LW-24OR0402015: “Complete analysis of attenuation and flux effects based on results from Zion beltline reactor pressure vessel materials.”

1. INTRODUCTION

The Zion Nuclear Generating Station was a decommissioned, two unit, Westinghouse 4-loop PWR facility, with each unit capable of producing 1,040 MWe. The units were commissioned in 1973, permanently shut down in 1998, and placed into SAFSTOR (a method of decommissioning where a nuclear facility is placed and maintained in a condition that allows the facility to be safely stored and subsequently decontaminated to levels that permit release for unrestricted use) in 2010. The Zion Unit 1 RPV was composed of the head, three ring or shell sections composed of hemispherical plates with two vertical welds, and a bottom plate. It had a total height without the head plate of approximately 419 inches (1,064 cm). The vessel wall had an inner diameter of 173 inches (439 cm) and a thickness of 8.8 inches (22.4 cm) over the beltline region. The nozzle ring section is approximately 11 inches thick. Including cladding, the reactor vessel weighed about 700,000 lbs. (317,515 kg) and had a total activity of about 400 curies [3].

The Zion Unit 1 RPV was cut using an oxy-propylene torch into 17 segments over four levels. As previously described [1, 2, 3], the Zion Unit 1 Beltline Weld Segment 1, with dimensions of ~ 13' x 6' (157.5" x 72.9" x 8.8") and containing the well-characterized WF-70 beltline weld and the base metal A533B heat B7835-1, was cut from just below the circumferential weld between the nozzle section and the intermediate shell. At the Energy Solutions MPF, Segment 1 was cut into blocks. A total of 5 blocks with base metal and two blocks of weld metal were cut out of Segment 1 [3]. Those blocks were sent to BWXT, Lynchburg VA, for specimen machining [4].

Assessments of the attenuation effects were made using weld metal data. Base metal data revealed a strong "surface" effect of the through thickness distribution of the mechanical properties. It is well known that the ductile-to-brittle transition temperature is lower at the surface layers of thick RPV plates, see [10] for example, than in the middle of the plate. The Zion Charpy T_{41J} and fracture toughness T_0 through thickness distribution confirmed that this effect continues to appear after irradiation as well.

The RPVs from several decommissioned power reactors have been sampled to examine the issue of mechanical property variations through the RPV thickness, and a few special-purpose test reactor experiments have been carried out to obtain insight into this same issue. The major studies are listed in Tables 1 and 2. These previous studies have demonstrated the difficulty of obtaining an unambiguous description of how the properties evolve in a thick section of steel under irradiation, particularly in the case of post-mortem examination of a decommissioned RPV. As reflected in the accepted embrittlement trend curves [11,12], radiation-induced embrittlement is known to be sensitive to a range of material and irradiation parameters, including neutron flux and fluence, irradiation temperature, alloy composition (including minor or "tramp" elements), and product form. Since it is the change in properties under irradiation that is of interest, the unirradiated properties also need to be known as a function of location in the vessel. The local alloy chemistry also needs to be known as a function of depth in both the irradiated and unirradiated materials. Local RPV chemistry cannot be measured prior to irradiation and the unirradiated material will at best be similar to that of the in-service component.

Table 1. Previous decommissioned power reactor RPV studies

Reactor	Country	Type	Shut down	Testing
JPDR	Japan	BWR	1976	1994-1999
Gundremmingen, Unit A	Germany	BWR	1977	~1988-1992
BR-3	Belgium	PWR	1987	1995-1999
Novo-Voronezh Unit 1	Russia	VVER	1984	1993-2000
Chooz-A	France	PWR	1991	1995-1999
Greifswald Unit 1	Germany	VVER	1990	2004-2012
Greifswald Unit 2	Germany	VVER	1990	2004-2012
Greifswald Unit 3	Germany	VVER	1990	2004-2012
Greifswald Unit 4	Germany	VVER	1990	2004-2012
Trawsfynydd	UK	Magnox	1991	1996-2002
Barsebäck 2	Sweden	BWR	2005	2019-2022

Table 2. Damage Attenuation Experiments.

Experiment title	Country	Approximate timeframe
IRL (T~60°C)	USA	early 1970s
ORR Pool Side Facility	USA	late 1970s
IAEA-NRI	Czech Republic	about 2002-2010

An excellent review of the major studies listed in Tables 1 and 2 can be found in Ref. [13], and references therein. Although in some cases the measured attenuation of embrittlement was generally consistent with the predictions of the attenuation model in the U.S. Regulatory Guide 1.99, Rev. 2 [11], many comparisons were confounded by local variations in the unirradiated mechanical properties. This variation can be best illustrated by the results obtained from the detailed characterization of the through-thickness properties of a beltline weld cut from a RPV that never went into service [14]. Importance of this example is that it is the same WF-70 weld that was used in Zion Unit 1 beltline weld. As shown in Fig. 1, the unirradiated 41J Charpy transition temperature varied by more than 40°C depending on the depth and which section of the weld has been tested. Similar variations confounded the interpretation of the post-mortem attenuation studies of the Gundremmingen Unit A RPV as shown in Fig. 2 [15].

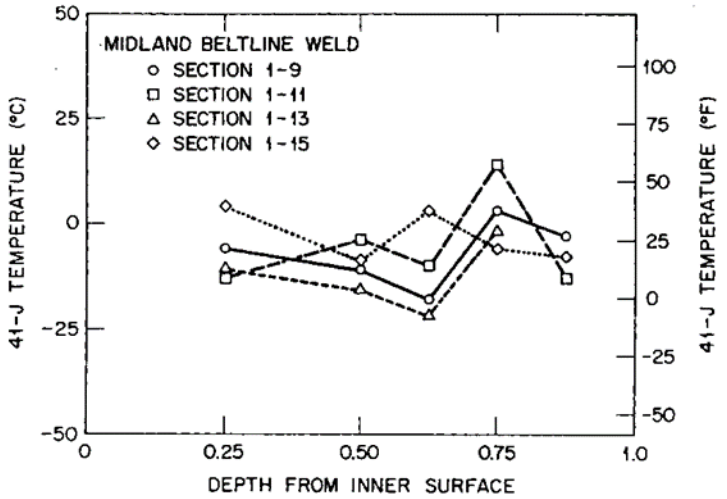

Figure 1. Through-thickness 41J Charpy impact results for the Midland beltline weld in unirradiated condition [14].

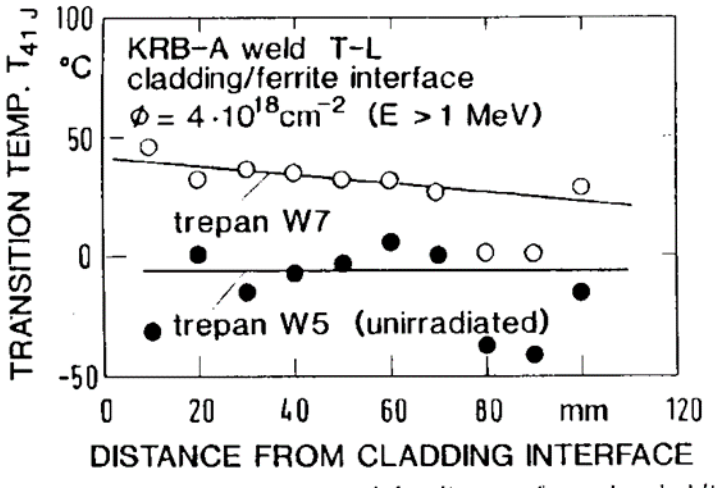

Figure 2. Through-thickness 41J Charpy impact results for the Gundermmingen Unit A weld in the unirradiated and irradiated conditions [15].

Although the attenuation experiments listed in Table 2 permitted better opportunities for characterization of the unirradiated materials and control of the experimental variables, the results were not as definitive as planned. As discussed in Ref. [13], the data was confounded by unexpected behavior, which was variously attributed to experimental uncertainties, unexplained sensitivities to alloy chemistry and Charpy specimen orientation, and what has been referred to as "anomalous results" [16]. For example, although the master curve data for the JRQ plate material irradiated in the IAEA-NRI experiment shown in Fig. 3 is generally consistent with the dpa-based attenuation model in ASTM E900, it exhibits higher than expected shifts in the 0.3 to 0.5T region and an anomalously high shift at about 0.25-T, where T was the simulated thickness of the vessel wall.

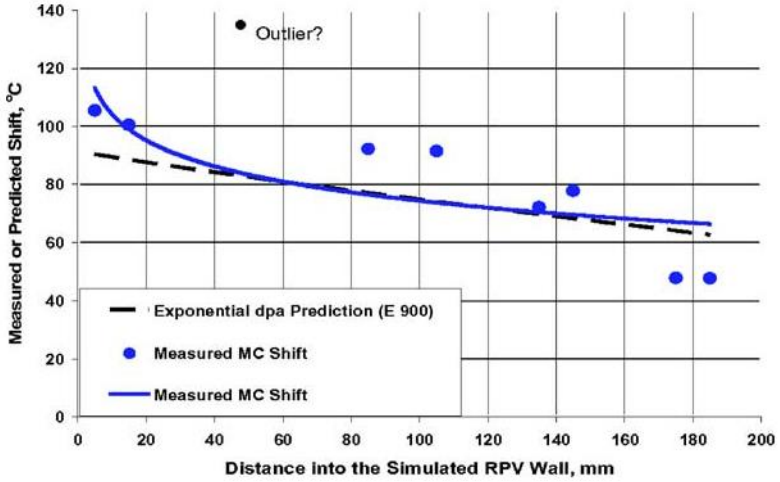

Figure 3. Predicted and measured values of Master Curve T_0 shift for the JRQ plate material [16].

Considering the data shown in Figs. 1-3, and other interpretational difficulties discussed in Ref. [13], it perhaps is not surprising that understanding the results of the current investigation of the Zion RPV remains a work in progress.

This report is prepared in satisfaction of Milestone M3LW-24OR0402015: "Complete analysis of attenuation and flux effects based on results from Zion beltline reactor pressure vessel materials."

2. THROUGH THICKNESS MECHANICAL PROPERTIES DISTRIBUTION OF ZION WELD METAL

For weld metal, all specimens were cut from one block of beltline weld, CF. Figure 4 shows a schematic cutting diagram of this block presenting the layers with various types of specimens. In the case of weld block CF, layers of Charpy blanks and 0.4T C(T) were alternated through the thickness of the weld. The weld had a V-shape profile with the narrowest portion being the closest to the inner surface of the vessel facing the reactor core. Some of the blanks were used to machine tensile specimens and multipurpose coupons as previously described for the base metal. Additionally, some of the blanks were machined outside our specification and were subsequently re-machined into other specimens for future considerations. Detail may be found in reference [5]. Charpy specimens of layer "I" were not tested. These specimens are reserved for future testing and evaluations.

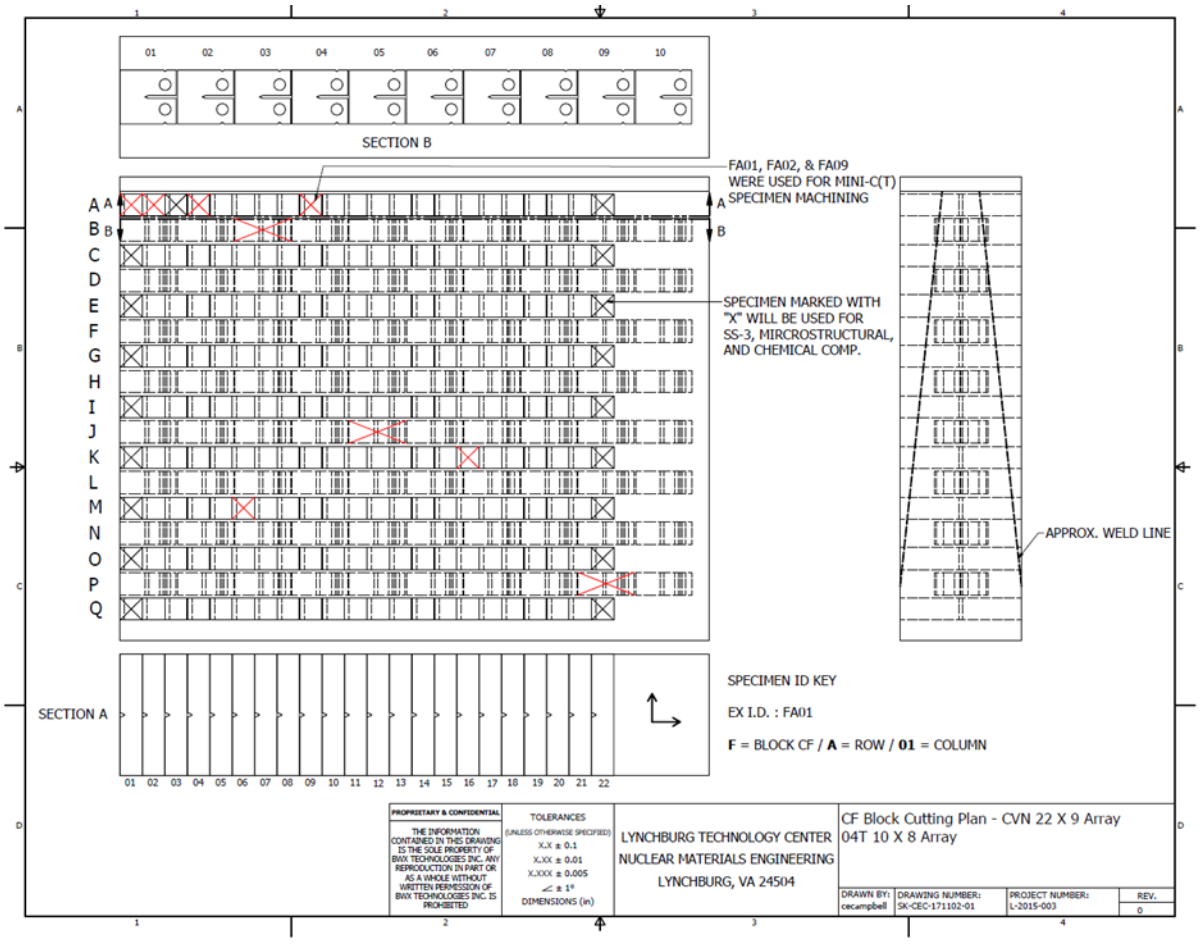

Figure 4. Block CF cutting plan showing alternating layers of Charpy and 0.4T C(T) specimens through the thickness of the vessel.

Figure 5 illustrates the distribution of the Zion beltline weld Charpy transition temperature, T_{41J}, through the thickness of the vessel wall. It appears that the absolute values of the T_{41J} do not significantly vary through the thickness of the wall until the very last layer. Moreover, layer 7, designated as "G" in Fig. 4, showed the highest T_{41J} temperature.

Figure 6 illustrates the distribution of the fracture toughness transition temperature of the beltline weld, T_0, through the thickness of the vessel. Like the Charpy 41-J transition temperature data shown in

Figure 5, the T_0 distribution did not exhibit a particular trend through the thickness of the vessel. Similarly to the Charpy layer 7 data, layers 8 and 10 exhibited higher fracture toughness T_0 values compared to other layers even though those layers are in the middle section of vessel wall.

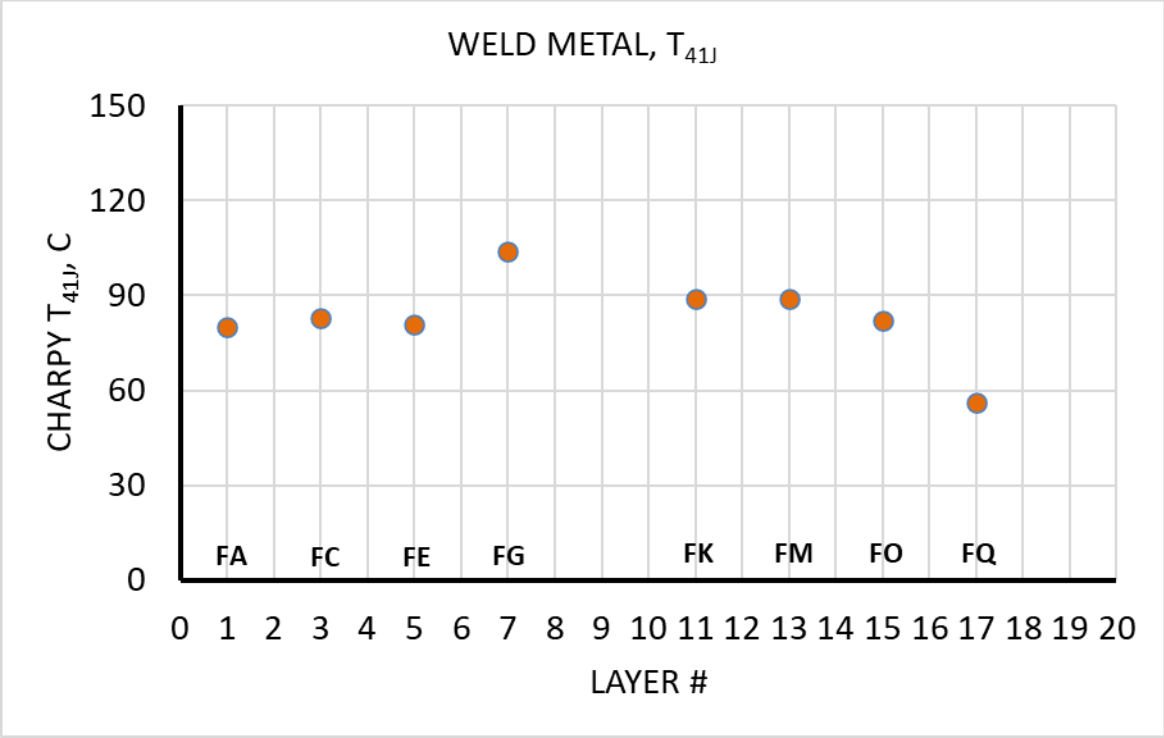

Figure 5. Distribution of the Charpy 41-J transition temperature of beltline weld metal through the thickness of the vessel wall. Layer 1 was closer to the reactor core.

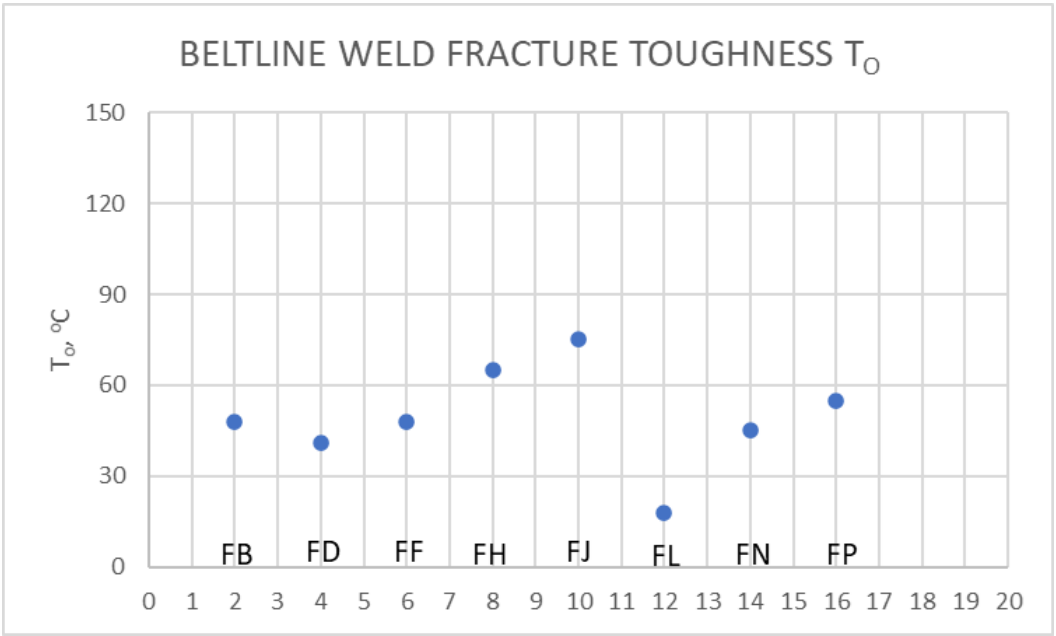

Figure 6. Distribution of the fracture toughness transition temperature, T_0, of beltline weld metal through the thickness of the vessel wall. Layer 1 was closer to the reactor core.

These unexpected “humps” in the transition temperature distributions were one of the main reasons to performed characterization of the archived material [8,9]. While the archive surveillance weld did not reveal any unusual behavior in the half-depth of the of the weld, it did show a very pronounced trend with T_0 distribution through the thickness of the weld, as seen in Fig. 7. This trend was used to calculate the shift of the fracture toughness transition temperature, T_0, through the thickness of the weld. Since it is well accepted fact that harpy and fracture toughness transition temperatures are following approximately the same trend, the same through-thickness dependence was used to calculate through-thickness distribution of Charpy T_{41J} transition temperature in the unirradiated condition using reported T_{41J} values for surveillance weld at ¼-thickess of the weld. Figure 8 represents the measured shift, ΔT, through the thickness of the vessel wall where blue points represent fracture toughness and red points represent Charpy transition temperatures, respectively.

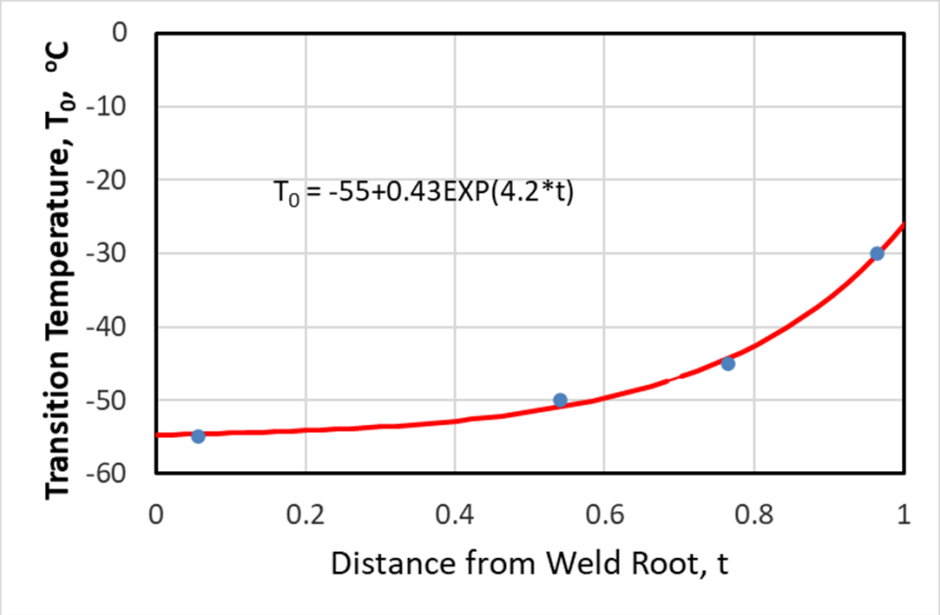

Figure 7. Through-thickness distribution of T_0 in the archived surveillance weld.

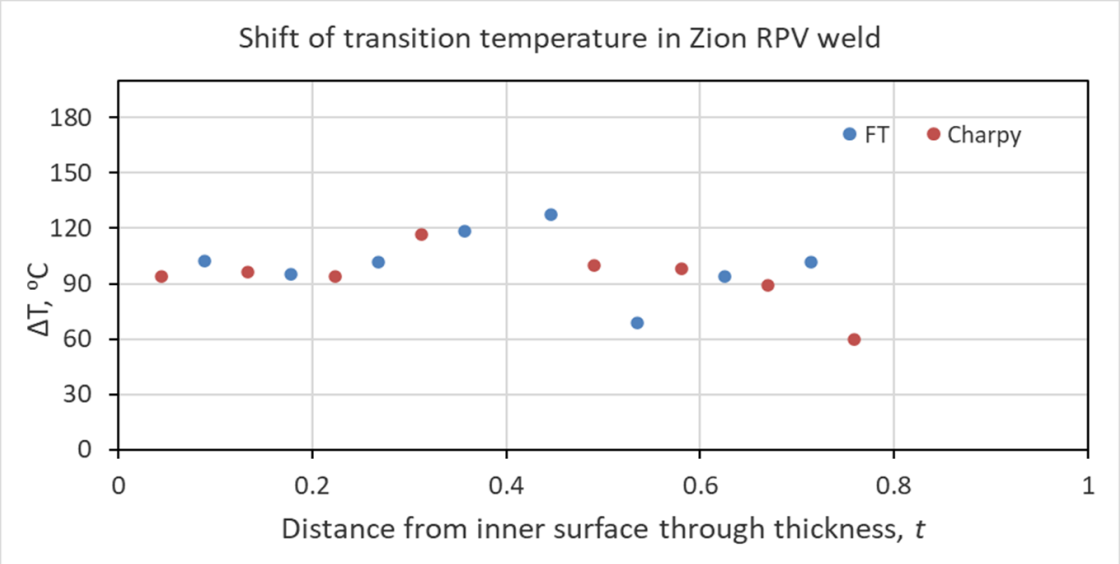

Figure 8. Shift of the fracture toughness (blue) and Charpy (red) transition temperature through the thickness of Zion RPV beltline weld.

3. MODELING ASSESSMENT OF ZION DATA

Since the change in mechanical properties of the Zion beltline materials did not follow the expected behavior as function of depth in the vessel, a previously developed computational model was used to investigate the potential reasons for this behavior. The development of the model and its application to RPV embrittlement was discussed in Refs. [17,18]. Briefly, the model simulates the radiation-induced evolution of point defect (vacancy and interstitial) clusters and copper-rich precipitates which give rise to hardening and embrittlement. The well-known reaction rate theory method is employed which permits the effects of parameters such as the neutron flux (atomic displacement rate) and irradiation temperature to be explicitly included. Relevant material parameters and the copper content are specified as input parameters.

As an example of the model behavior, Fig. 9 provides representative results from the model for matrix hardening as a function of displacement rate at 288°C at a total dose of 0.01 dpa, which is similar to the maximum does on the Zion RPV materials. The values shown in the figure can be converted to yield strength change and Charpy shift using standard conversions as discussed in [18], but it seems more suitable to focus on the parameters calculated directly by the model for the purpose of this illustration. Values are shown for the three defect types mentioned above, along the total hardening based on the root sum-of-squares (RSS) of the individual components. The potential impact of a reduced displacement rate (neutron flux) as a function of depth into the RPV can be inferred from this figure. For values typical of RPV materials, hardening from point defect clusters decreases and hardening from copper-rich precipitates increases as the displacement rate decreases. Because of the opposing effect of displacement rate on different types of defects, the total hardening can either increase or decrease with damage rate. The displacement rate at which the minimum in total hardening occurs will be a function of alloy composition and other material and irradiation parameters.

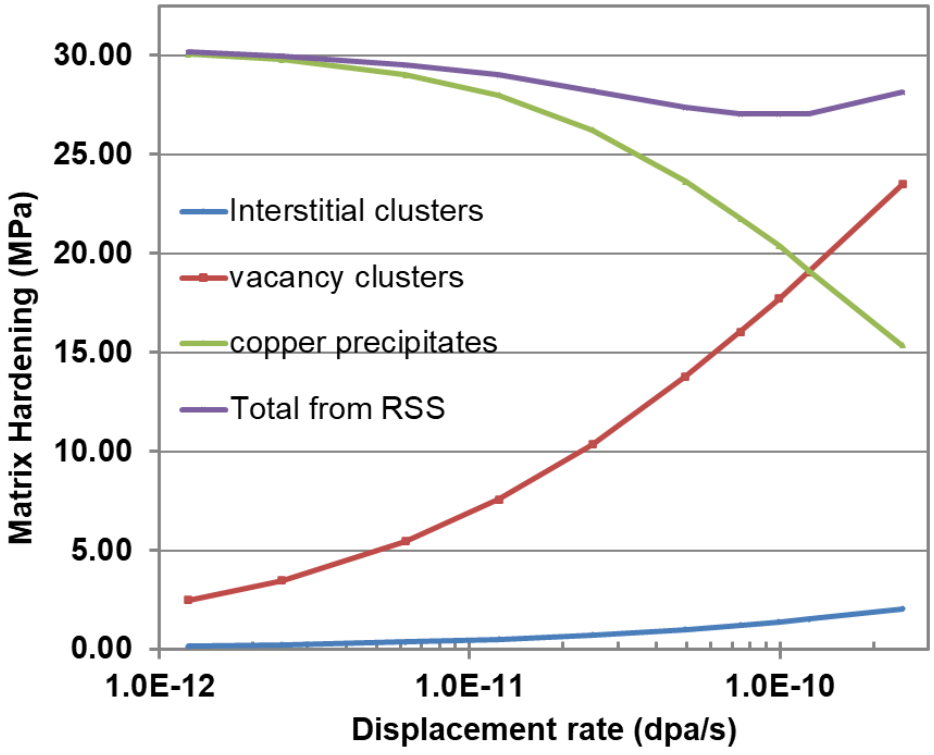

Figure 9. Predicted hardening for different microstructural defects for irradiation at 288ºC to 0.01 dpa. Copper content is 0.3 atom-%.

However, the results shown in Fig. 9 are for a constant total dose, which does not represent the through-thickness dose behavior obtained in an RPV. Fig. 10 shows the expected attenuation in an 8.8-inch thick RPV; the exponential attenuation formula from Regulatory Guide 1.99/2 [11] is compared with what is denoted as "real" dpa based on detailed transport calculations [19]. As pointed out previously [20], the dpa attenuation through the RPV is slower than that predicted by the NRC exponential model. However, attenuation is relatively strong in both cases and the relative attenuation is similar at the ¾-T position.

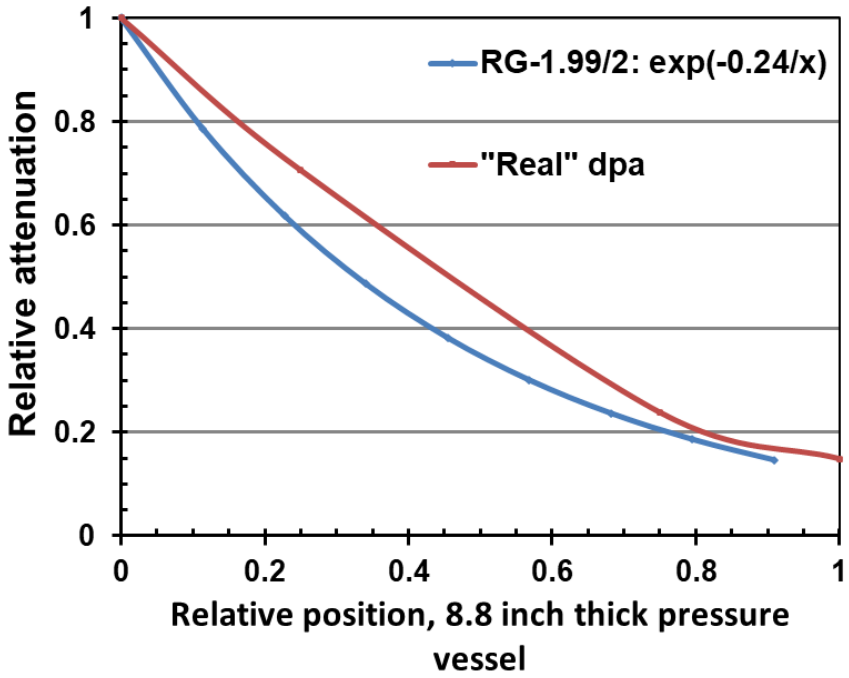

Figure 10. Relative attenuation of displacement rate through RPV. A comparison of the RG-1.99/2 attenuation model with neutron transport calculation ("real" dpa).

It is important to point out that it is not proper to assume that the attenuation in mechanical properties will be the same as the attenuation in the primary damage term, i.e. the atomic displacement rate. This is another way of saying that damage accumulation is not simply linear in damage formation. The difference is clear when comparing the results from Fig. 10 with those in Fig. 11. Although Fig. 10 indicates that total dose is reduced to about 20% at the ¾-T position, applying this reduction in the RG-1.99/2 embrittlement trend curve leads to ~40% of the predicted embrittlement. Application of the ASTM E900 embrittlement trend curve [12] with the same dose values indicates even less attenuation.

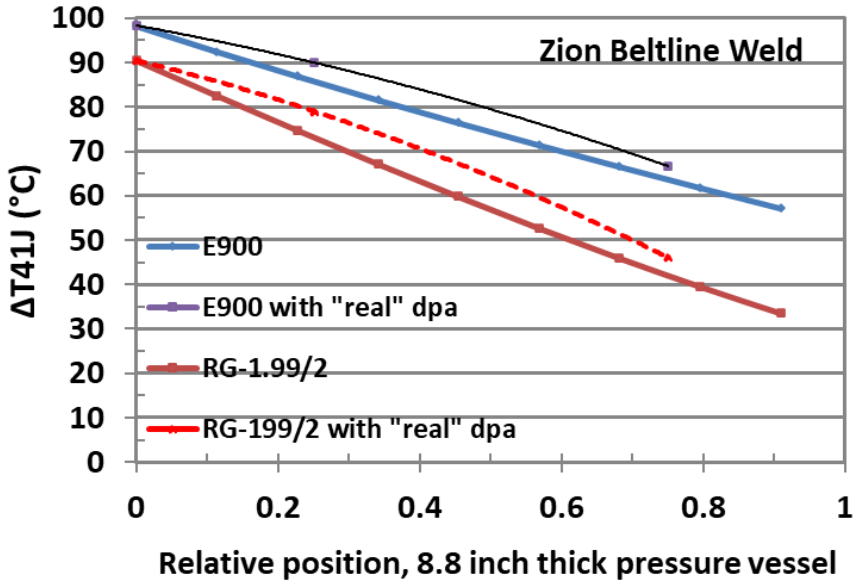

Figure 11. Attenuation of Charpy 41J transition temperature shift estimated for Zion beltline weld with different embrittlement trend curves.

The predictions of the microstructural model are consistent with the experimentally based embrittlement trend curves. This is shown in Fig. 12 in which results of the RG-1.99/2 trend curve are compared with model predictions obtained using two alternate parameter sets. The case with the higher assumed copper precipitate density and surface energy favors leads to greater embrittlement near the inside surface and more rapid attenuation. The case with a lower precipitate density and surface energy has a lower maximum value of Charpy shift and slower attenuation. The cross-over in the two predicted curves at about 0.65-T is related to the displacement rate change and the balance between point defect hardening and precipitate hardening as discussed with respect to Fig. 8 above.

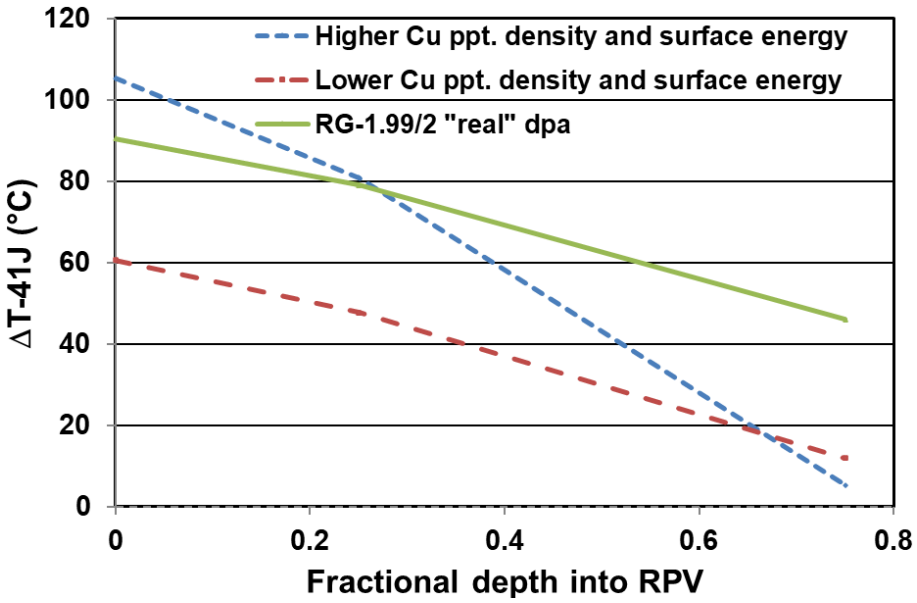

Figure 12. Comparison of Charpy 41J transition temperature shift estimated for the Zion beltline weld with microstructural model and the RG-1.99/2 embrittlement curve.

A variety of material and irradiation parameters were investigated using both the embrittlement trend curves and the microstructural models in attempt to understand the behavior of the Zion beltline materials. For example, the copper and nickel contents of individual samples was used as opposed to the nominal average values to see their impact on the results obtained with the RG-1.99/2 trend curve. The results are shown in Fig. 13, where the lower copper values measured between about 0.25-T and 0.5-T [8] would lead to lower Charpy shifts in the region where the measured values are higher.

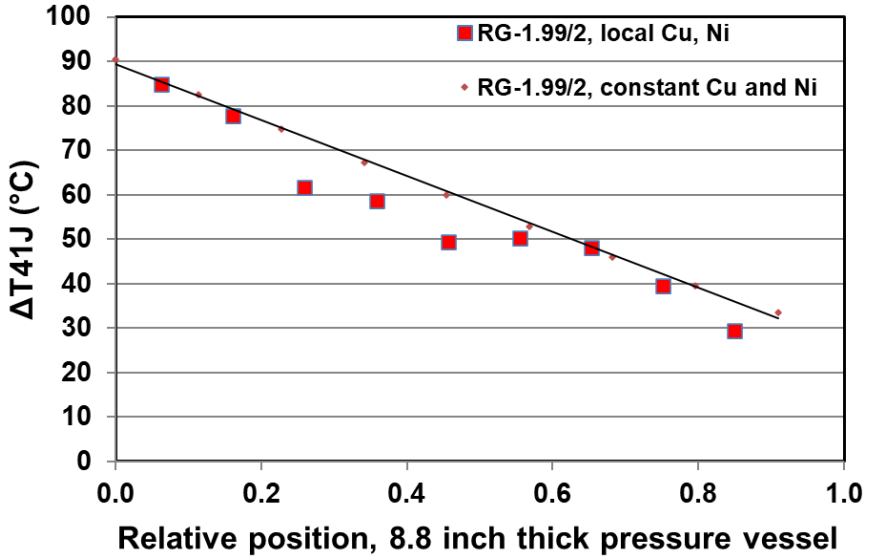

Figure 13. Comparison of Charpy shift estimated with RG-1.99/2 embrittlement trend curve using both local and nominal chemistry values.

The results of the computational and modeling analysis failed to provide any insight into the why the observed mechanical property changes deviated so significantly from the expected behavior. The simulations obtained using the microstructural model were broadly consistent with the embrittlement trend curves developed by the nuclear industry, and both were inconsistent with the Zion data as summarized in Fig. 14.

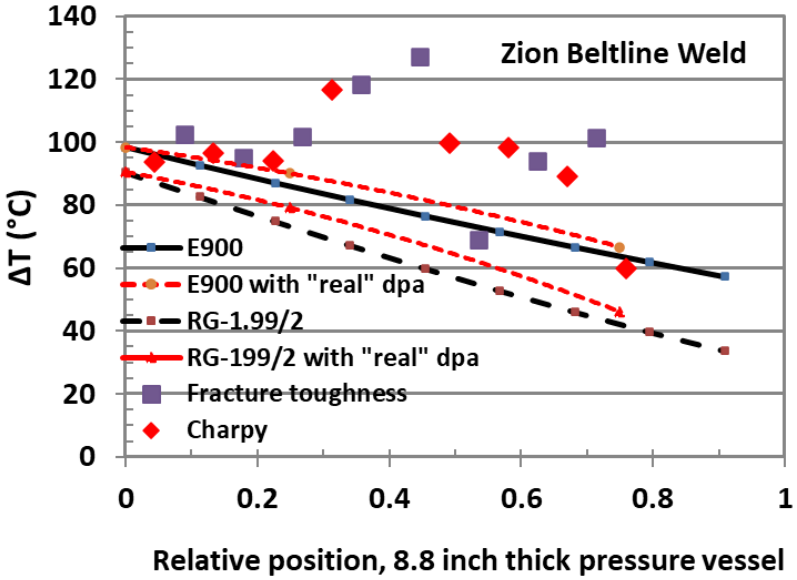

Figure 14. Comparison of Charpy and fracture toughness transition temperature shifts for Zion beltline weld with variants of embrittlement trend curves.

4. DISCUSSION AND CONCLUSIONS

The Zion beltline data appears to be quite inconsistent with our current understanding of damage mechanisms in RPV steels. In particular, the apparent increased embrittlement observed at depths between 0.2-T and 0.6-T shown in Fig. 14 is difficult to rationalize. To help clarify this unusual behavior, it is suggested to perform high temperature annealing (~ 500^{o}C) and testing of some remaining weld material to determine transition temperature of these annealed specimens at various thickness of the vessel to ensure that this behavior was or was not caused by through-thickness abnormalities prior to vessel operation. Together with the previous unexplained data on damage attenuation observed on some other RPVs discussed above, it seems clear that that further research is needed to make it possible to confidently predict the mechanical properties as a function of depth into the RPV.

5. REFERENCES

1. Rosseel, T. M., Sokolov, M., Nanstad, R. K., "Report on the Harvesting and Acquisition of Zion Unit 1 Reactor Pressure Vessel Segments," ORNL/TM-2016/240, June 2016.
2. Rosseel, T. M., Sokolov, M. A., Chen, X., Nanstad, R. K., "Zion Unit 1 Reactor Pressure Vessel Sample Acquisition: Phase 2 and Phase 3 Status Report," ORNL/TM-2016/561, September 2016.
3. Rosseel, T. M., Sokolov, M. A., Chen, X., Nanstad, R. K., "Transfer of Zion Unit1 Reactor Pressure Vessel Segment Blocks from the Cutting Vendor to the Machining Vendor," ORNL/TM-2016/240, January 2017.
4. Rosseel, T. M., Sokolov, M. A., Chen, X., Nanstad, R. K., "Report on the Completion of the Machining of Zion Unit 1 Reactor Pressure Vessel Blocks into Mechanical and Microstructural Test Specimens and Chemical Analysis Coupons," ORNL/TM-2018/861, May 2018
5. Sokolov, M.A, Rosseel, T.M, Edmondson, P., Chen, X., Nanstad, R.K., Manneschmidt, E.T., "Report of Preliminary Testing and Evaluation of Harvested Zion Unit 1 Vessel Beltline Weld and Base Metal Properties to Develop Insights into Neutron Attenuation, Material Variability, and Degradation of Ex-Service Reactor Pressure Vessel Materials," ORNL/TM-2019/1221, July 2019.
6. Sokolov, M.A., Chen, X., Rosseel, T. M., Manneschmidt, E.T., "Report on Fracture Toughness Testing Results and Evaluation of Harvested Zion Unit 1 Vessel Beltline Weld and Base Metal Materials," ORNL/TM-2020/1651, September 2020
7. Sokolov, M.A., Manneschmidt, E.T., and McAlister, M.R., "Mechanical Testing of the Harvested and Archival Zion Beltline Materials," ORNL/SPR-2021/2237, September 2021.
8. Sokolov, M.A., Manneschmidt, E.T., and Reed, J., "FRACTURE TOUGHNESS RESULTS OF ARCHIVAL ZION BELTLINE WELD MATERIAL IN SUPPORT OF CHARACTERIZATION OF THE HARVESTED BASELINE MATERIALS," ORNL/SPR-2022/2562, August 2022.
9. Sokolov, M.A., and X. Chen "Though thickness characterization of archived Zion weld metal", ORNL/SPR-2024/3562, August 2024.
10. Stelzman, W.J, Berggren, R.G., and Jones, T.N., "ORNL Characterization of Heavy-Section Steel Technology Program Plates 01, 02, and 03," ORNL/TM-9491, NUREG/CR-4092, April 1985.
11. "Radiation Embrittlement of Reactor Vessel Materials," Regulatory Guide 1.99, Revision 2, U.S. Nuclear Regulatory Commission, May 1988, available from the U.S. National Technical Information Service, Springfield, VA.
12. ASTM E900-21, Standard Guide for Predicting Radiation-Induced Transition Temperature Shift in Reactor Vessel Materials, ASTM International, West Conshohocken, PA.
13. English, C., and Server, W., "Attenuation in U.S. RPV Steels," EPRI Materials Reliability Program (MRP-56), Electric Power Research Institute, Palo Alto, CA, June 2002.
14. R. K. Nanstad, D. E. McCabe, and R. L. Swain, "Evaluation of Variability in Material Properties and Chemical Composition for Midland Reactor Weld WF- 70," Effects of Radiation on Materials, STP 1325, R. K. Nanstad, M. L. Hamilton, F. A. Garner, and A. S. Kumar, Eds., American Society for Testing and Materials, West Conshohocken, PA, 1999, pp. 125-156.
15. Kussmaul, K, Föhl, J., and Weissenberg, T., "Investigation of Materials from a Decommissioned Reactor Pressure Vessel—A Contribution to the Understanding of Irradiation Embrittlement," Effects of Radiation on Materials: 14th International Symposium (Volume II), ASTM STP 1046, N. H. Packan, R. E. Stoller, and A. S. Kumar, Eds., ASTM International, West Conshohocken, PA, 1990, pp. 80-104.
16. Server, W., Brumovský, M., Kytka, M., Soneda, N., and Spanner, J., "Further Results on Attenuation of Neutron Embrittlement Effects in a Simulated RPV Wall," Journal of ASTM International 7 (2010) JAI102070.
17. Stoller, R.E. "The Influence of Damage Rate and Irradiation Temperature on Radiation-Induced Embrittlement in Pressure Vessel Steels," Effects of Radiation on Materials, 16th International Symposium, ASTM STP 1175, A. S. Kumar, D. S. Gelles, R. K. Nanstad, and E. A. Little, Eds., American Society of Testing and Materials, Philadelphia, 1993, 394-426.

18. Stoller, R.E. “Pressure Vessel Embrittlement Predictions Based on a Composite Model of Copper Precipitation and Point Defect Clustering,” Effects of Radiation on Materials, D. S. Gelles, R. K. Nanstad, A. S. Kumar, and E. A. Little, Eds., ASTM STP 1270, American Society of Testing and Materials, Philadelphia, 1996, pp. 25-59.
19. Albert, T.E., Gritzner, M.L., Simmons, G.L., and Straker, E.A. “PWR and BWR Radiation Environments for Radiation Damage Studies, “EPRI NP-152, Electric Power Research Institute, Palo Alto, CA, September 1977.
20. Stoller, R.E., and Greenwood, L.R., “An Evaluation of Through-Thickness Changes in Primary Damage Production in Commercial Reactor Pressure Vessels,” Effects of Radiation on Materials, S. T. Rosinski, M. L. Grossbeck, T. R. Allen, and A. S. Kumar, Eds., ASTM STP 1405, American Society of Testing and Materials, West Conshohocken, PA, 2001, pp. 204-217.